VSP

Journal of Biomaterials Science 23 (2012) 405–424

Journal of BIOMATERIALS SCIENCE
brill.nl/jbs

A Viscoelastic Chitosan-Modified Three-Dimensional Porous Poly(L-Lactide-co-ε-Caprolactone) Scaffold for Cartilage Tissue Engineering

Chao Li [a], **Lili Wang** [a], **Zheng Yang** [b], **Gonhyung Kim** [c], **Haifeng Chen** [a] **and Zigang Ge** [a,d,*]

[a] Department of Biomedical Engineering, College of Engineering, Peking University, Beijing 100871, P. R. China

[b] Tissue Engineering Program, Life Sciences Institute, National University of Singapore, 117510 Singapore

[c] Department of Veterinary Surgery, College of Veterinary Medicine, Chungbuk National University, Cheongju 361763, South Korea

[d] Center for Biomaterials and Tissue Engineering, Academy for Advanced Interdisciplinary Studies, Peking University, Beijing 100871, P. R. China

Received 12 July 2010; accepted 14 December 2010

Abstract

Biomaterials have been playing important roles in cartilage regeneration. Although many scaffolds have been reported to enhance cartilage regeneration, none of the scaffolds available are optimal regarding mechanical properties, integration with host cartilage and providing proper micro-environment for chondrocyte attachment, proliferation and differentiation. In the current study, chitosan-modified poly(L-lactide-co-ε-caprolactone) (PLCL) scaffolds were fabricated to simulate the main biochemical components of cartilage, as well as their interaction with the aim to endow them with viscoelasticity similar to native cartilage. Porous PLCL scaffolds were fabricated with porogen-leaching, freeze-extraction and freeze-gelation before chitosan was cross-linked. The acquired porous scaffolds had pore sizes ranging from 200 to 500 μm and about 85% porosity with good interconnection between individual pores. Chitosan was successfully cross-linked to PLCL scaffolds, as validated by ninhydrin staining and X-ray photoelectron spectroscopy (XPS). The viscoelasticity of the scaffolds was similar to that of bovine cartilage and they had a relatively good recovery ratio from compression deformation, while the Young's modulus was one order of magnitude less than cartilage. Not only could the chitosan-modified PLCL scaffolds promote cell adhesion and proliferation, but also they could significantly enhance excretion of aggrecan and type-II collagen, as testified by both histology and quantitative PCR, compared with PLCL scaffolds. With the fabrication of biomimetic scaffolds, it is possible to make scaffolds for cartilage tissue engineering, which are not only biocompatible, but also have mechanical properties similar to native cartilage.

* To whom correspondence should be addressed. Tel.: (86-10) 6275-6736; Fax: (86-10) 6275-7545; e-mail: zigang.ge@gmail.com

DOI:10.1163/092050610X551970

Keywords
Cartilage tissue engineering, PLCL, chitosan, biomimetic, viscoelasticity

1. Introduction

Progress in cartilage tissue engineering is relatively slow, compared with bone tissue engineering. Many reasons contribute to this disparity, such as poor blood and nerve supply, lack of adult stem cells or progenitor cells, existing chondrocytes' inferior ability to proliferate, complex physiological mechanical environment, and poor integration between *de novo* cartilage and host cartilage [1]. Autologous chondrocyte implantation (ACI) has been a powerful tool to deal with focal cartilage defects of young patients [2, 3], while arthroscopic lavage, abrasion arthroplasty, subchondral drilling and microfracture all lead to inferior regeneration [3]. Biomaterials and scaffolds have been playing constructive roles in cartilage regeneration in the forms of micrometer-scale beads as platform of cartilage formation [4], as cell-carrying vehicles of autologous chondrocyte implantation [5], as scaffolds to trap living cells *in vivo* [6], or as supporting structures, as well as integration with host cartilage [7]. Individual scaffolds have been fabricated with pre-designed properties to account for one or several challenges faced by cartilage regeneration. The mechanical properties of scaffolds are one of the most challenging issues faced by *de novo* cartilage. During both original and degradation stages, the difference between the mechanical properties between neo-cartilage (or scaffolds) and host cartilage often leads to the deterioration of neo-cartilage during daily joint movement.

Although the importance of mechanical compliance of scaffolds with native cartilage has long been recognized, few of the existing scaffolds meet the requirement. Proper elastic properties similar to surrounding natural cartilage are critical for scaffolds used for cartilage regeneration and cyclic mechanical stimuli could regulate the phenotype of chondrocytes through three-dimensional scaffolds [8]. Several biodegradable elastomers have been synthesized, such as poly(1,8-octanediol citrate) (POC), poly(glycerol sebacate) (PGS) and poly(L-lactide-co-ε-caprolactone) (PLCL) (molar ratio 7:3), which were proven to be potentially better suited for use as a biodegradable scaffold to improve the quality of engineered cartilage when applying long-term cyclic compression on the cell–scaffold construct *in vitro* [9]. PLCL is a highly elastic biodegradable polymer with a relatively mild degradation, which avoids abrupt pH value drops like those reported in PLA and PGA scaffolds [10–12]. It can be used to simulate the elastic collagen in the extracellular matrix of native cartilage.

Biochemical factors are also very important for cartilage regeneration. Although the fabricated PLCL scaffolds could transfer external mechanical signals to cells attached to them through their high elasticity, they usually lack the necessary microenvironment for cell differentiation [13–15]. Chitosan is a derivative of a natural macromolecular compound easily obtained and has been broadly applied to tissue engineering due to its relatively good biocompatibility and ease of use. Since

chitosan possesses highly reactive amine groups in its structure, it could be easily modified or cross-linked to other functional macromolecules by applying various treatments. Chitosan can be regarded as a biochemical counterpart of glycosaminoglycans (GAGs, the main components of proteoglycan) due to its similar hexose consisting of water-soluble structure units [16, 17]. So far, the most promising result arises from three-dimensional woven polyglycolic acid (PGA) yarns mixed with hydrogel, which has shown mechanical similarity with native cartilage, regarding tensile stress, tensile strain, aggregate modulus, hydraulic permeability and Young's modulus [18]. However, in this system the hydrogel was simply mixed with a woven structure to serve as a cell-carrying vehicle and material coating instead of integration with main structures to contribute to mechanical properties of the scaffolds accordingly. Furthermore, this strategy does not mimic natural biochemical components and properties of cartilage, so it is hard to further improve and modify mechanical properties through adjusting the fabrication strategy accordingly.

Within native cartilage, stiff and elastic cross-linked collagen helps cartilage to resist lateral expansion on axial compression by maintaining an original framework. GAG or aggrecan, intimately attached to collagen, holds large amounts of ions and water *via* negative charges. Upon considerably increased compression, some water molecules are forced out, causing reversible deformation of cartilage and temporarily increasing the contact area, while most water molecules are pressured and remain at their original location by GAG, contributing to the compression stiffness and lubrication of cartilage [19]. Cartilage can be regarded as a biphasic material with complex mechanical properties, such as anisotropy, nonlinearity and viscoelasticity [20]. As a weight-bearing tissue, articular cartilage, as well as scaffolds implanted to regenerate cartilage, face challenges to maintain structural integrity under continuous complex mechanical loads. Viscoelasticity is one of the most important mechanical properties of cartilage. In the current study, bi-phasic viscoelastic porous scaffolds were fabricated by simulating natural components of cartilage, collagen, aggrecan and their interaction, in an aim to make scaffolds with mechanical properties similar to native cartilage. Elastic PLCL was briefly used as basal material of scaffolds, while hydrophilic chitosan was cross-linked to PLCL using the aminolysis method to provide bi-phasic structure. Ninhydrin staining and X-ray photoelectron spectroscopy (XPS) were done to confirm the immobilization and distribution of chitosan. Mechanical properties (compression and viscoelasticity) were evaluated, and chondrocyte behavior in the scaffolds, including adhesion, proliferation and excretion of aggrecan and type-II collagen, was investigated.

2. Materials and Methods

2.1. Fabrication of the PLCL Scaffold

A combination of porogen-leaching, freeze-extraction and lyophilization was adopted to fabricate three-dimensional scaffolds, as described previously [21]. Briefly, PLCL (LA/CL = 7:3; M_w 23 000; purchased from Daigang Biomaterials)

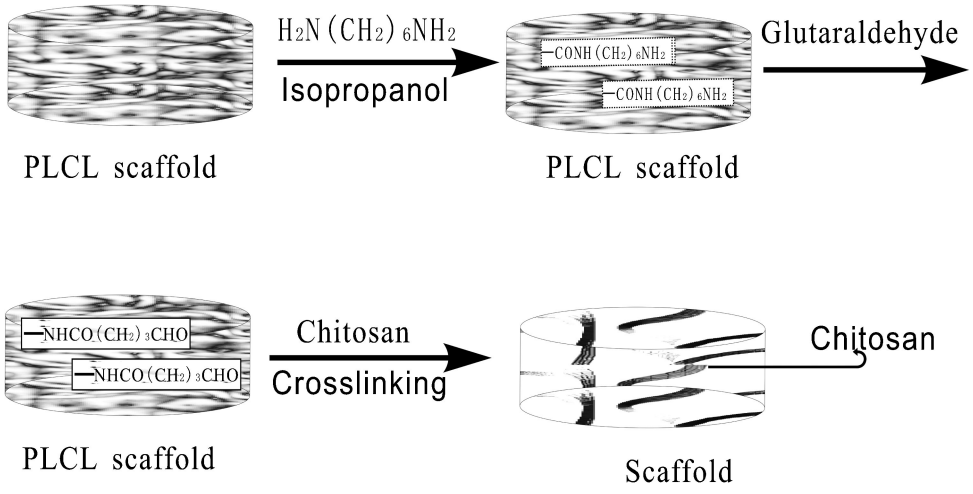

Figure 1. Scheme of the chemical reaction of the immobilization of chitosan onto the PLCL scaffold.

was dissolved in 1,4-dioxane (10%, w/v) and mixed with a proportional amount of NaCl. After agitation, the NaCl/PLCL mixtures were cast in glass molds and then frozen at −20°C for 24 h. The frozen mixtures were immersed in a 70% ethanol aqueous solution for 72 h that was pre-cooled to −20°C. After the solvent and part of NaCl were substituted with ethanol aqueous solution, the NaCl/PLCL mixtures were lyophilized in a freeze dryer for 24 h before being rinsed with distilled water to remove NaCl. PLCL scaffolds were frozen at −20°C, before being lyophilized for another 24 h, and stored in a desiccator until use.

2.2. Aminolysis of the PLCL Scaffold and Chitosan Immobilization

An aminolysis method was used to immobilize chitosan (degree of deacetylation 80.0–95.0%, viscosity 50–800 mPa · s; Guoyao Chemical Reagents) in the PLCL scaffolds as described previously [22] (Fig. 1). The scaffolds were immersed in a 50% ethanol solution for 2 h to remove any oil on the scaffold surface, before being dried and immersed in a 10% (w/v) 1,6-hexanediamine/isopropanol solution at 37°C for 10 min and rinsed with distilled water. The scaffolds were then immersed in a 1% glutaraldehyde solution at room temperature for 3 h before being rinsed with distilled water. The scaffolds were incubated in 2 mg/ml chitosan solution (pH 3.5) at 2–4°C for 24 h, then rinsed with 0.1 M acetic acid solution before being rinsed with distilled water. The acquired scaffolds were left to dry in the vacuum chamber and were stored in a dessicator until further use. All the procedures were undertaken in a vacuum chamber to ensure complete penetration of the solution into the whole scaffolds for a thorough reaction.

2.3. Characterization of the Scaffolds

The scaffolds were sectioned with a lancet, fixed on conductive adhesive and coated with gold for 80 s at 18 mA, before the surface and cross-section morphology of the

scaffolds were observed by scanning electron microscopy (SEM; Quanta 200FEG, FEI) at an accelerating voltage of 15 kV.

Distribution of amine groups in modified PLCL scaffolds was evaluated by ninhydrin staining. Briefly, the scaffolds were immersed in 1.0 M ninhydrin/ethanol solution for 1 min, before being transferred into a glass tube and incubated at 80°C for 10 min to accelerate the reaction. The photographs of the scaffolds were taken with a Sony digital camera (DSC-H200).

Immobilization of chitosan onto the PLCL scaffolds was confirmed by X-ray photoelectron spectroscopy (XPS) (AXIS-Ultra, Kratos Analytical). XPS was performed using monochromatic Al K_α radiation (225 W, 15 mA, 15 kV). The operating pressure during analysis was maintained at about 10^{-9} Torr. To compensate for surface charge effects, binding energies were calibrated using the C_{1s} hydrocarbon peak at 284.80 eV.

2.4. Swelling Ratio and Porosity

Freeze-dried scaffolds were immersed in phosphate-buffered saline (PBS) at 37°C for 2 h until equilibrium of swelling was reached. The swollen scaffolds were taken out and immediately weighed with a microbalance after the excess water on the surfaces of the scaffold was carefully removed with tissue paper. The swelling ratio was calculated and expressed as ER (ER $= (W_s - W_d)/W_d$, where W_s and W_d are the weight of the swollen and dried scaffolds, respectively).

Porosity was estimated with a similar methodology [23]. The exact sizes of the scaffolds were measured with a vernier caliper, while the mass of the scaffolds was taken carefully. The scaffolds were immersed in absolute alcohol for 2 h before weighted again. Porosity was calculated as $(W_s - W_d)/(\rho/V)$, where ρ is the density of alcohol and V the volume of the scaffolds, respectively.

2.5. Mechanical Tests

A compression test creep test, and stress relaxation test of the scaffolds were undertaken with bovine articular cartilage as the control. Fresh quadrate bovine articular cartilage explants (10 mm × 10 mm) were harvested from the weight-bearing area of the femoral head of bovines and kept wet with PBS before testing. All PLCL scaffolds, chitosan-modified PLCL scaffolds and cartilage explants were immersed in PBS for 24 h at room temperature prior to testing. The length, width and thickness of the samples were measured with a vernier caliper and 6 tests were performed for each group.

2.5.1. Compression Test

An unconfined compression test was carried out with an Instron 5843 mechanical test instrument. Compressive loads were applied to individual specimen in a PBS bath using a stainless steel indenter. All the samples were pre-loaded three times to a 10% strain before a constant loading at a displacement of 0.5 mm/min until 45% strain was reached. The measured thickness was converted to the strain of the

sample ($\varepsilon = 1 - (L/L_0)$, where L_0 and L are the thickness before and after compression, respectively). Young's modulus ($E = \sigma/\varepsilon$, where σ and ε denote the stress and strain of the sample respectively) was determined directly on a Instron 5843. The thickness of each scaffold was measured to calculate the compressive recovery ratio within 1 min after removal of the compressive load. The recovery ratio was used to assess the capability of the scaffolds to recover from the deformation and expressed as recovery ratio (recovery ratio $= L_1/L_0$, where L_1 and L_0 are the final and initial thickness of the scaffolds after and before compression, respectively).

2.5.2. Creep Test

Creep experiments were carried out using an Electronic Universal Testing Machine (WDW3020) in a static unconfined compression. The samples with precompression treatment were loaded at 10 kPa, and the strain was recorded continuously at specified time intervals for 300 s.

2.5.3. Stress Relaxation Test

A stress relaxation test was performed using an Electronic Universal Testing Machine (WDW3020) under a constant strain. After the samples were compressed to 20 and 30% of the original thickness, the strain was maintained, and the resulting stress values were recorded over time for 600 s.

2.6. Chondrocyte Culture

Chondrocytes (C28-I2; 15–20 passages), kindly provided by Mary Goldring at Children's Hospital Boston, were cultured in tissue culture polystyrene (TCPS, Costar) with culture medium (Dulbecco's modified Eagle medium (DMEM, Gibco)) containing 10% fetal bovine serum (FBS), 100 IU/ml penicillin and 100 μg/ml streptomycin (Gibco) at 37°C in 5% CO_2/95% air.

2.6.1. Biocompatibility

3-(4,5-Dimethyl-2-thiazolyl)-2,5-diphenyl-2H-tetrazolium bromide (MTT, M 2128, Sigma) was applied to evaluate the biocompatibility of the scaffolds at 24 and 48 h, respectively, with TCPS wells as positive the control and latex rubber (Haimen Yangzi Medical) as the negative control. Test materials were cut into $5 \times 5 \times 2$ mm samples and sterilized in 70% ethanol aqueous solution for 2 h before being air-dried and sterilized under UV light for 30 min. The scaffolds were then rinsed and immersed in PBS for another 30 min. Chondrocytes (5000 cells/well) were cultured in a 96-well plate with and without the test materials. MTT solution (100 μl, 5 mg/ml) was added in each well at 24 and 48 h, respectively, and incubated at 37°C for 3 h. All wells were emptied before 150 μl DMSO was added. Optical density at 540 nm wavelength was measured to determine the percentage of viable cells. The value was compared and expressed as a percentage of the data on the TCPS wells. Six samples from each group were measured.

2.6.2. Cell Attachment and Proliferation

Proliferation of chondrocytes within scaffolds was evaluated quantitatively with Hoechst 33258 (H6024, Sigma). DNA content was analyzed after chondrocytes

were seeded onto the scaffolds (5 × 5 × 2 mm) for 6 h (for cell attachment) and 3 days (for cell proliferation). Cell suspension was added drop-wise onto the top of the scaffold at a density of 2×10^5 cells/scaffold in 500 µl culture medium (DMEM medium with 10% FBS). Culture medium was carefully added to the Petri dish (12 wells, Costar) to cover the scaffolds after 30 min incubation. For analysis, cells on the scaffolds were digested in 3 mg/ml proteinase K (H10091, Merck) overnight at 57°C. H33258 in TRIS-EDTA · 2Na (TNE) buffer (0.1 µg/ml) was used to dye the digested solution which was loaded in black 96-well plates. Blanks and a series of DNA standards were also loaded in order to permit calibration of the fluorescence reading. Fluorescence intensity was measured on a microplate reader at excitation and emission wavelengths of 360 and 465 nm, respectively. A calibration curve was obtained from DNA standard solutions with known concentrations. The DNA concentration is proportional to the cell number because each cell has a fixed DNA content. Therefore, the DNA concentrations provide a reliable means for comparing the cell numbers grown on the chitosan-modified PLCL scaffolds and plain PLCL scaffolds. Four repeats for each sample were averaged.

2.6.3. Cell Distribution and Morphology

Distribution and morphology of cells on the scaffolds were observed by confocal laser scanning microscopy (CLSM, LSM510, Zeiss). After the chondrocytes seeding for 6 h and 3 days, cell-seeded scaffolds were rinsed three times in PBS and incubated with 100 µl of 2 µg/ml Fluorescein Diacetate Solution (FDA, F7378, Sigma) at 37°C for 15 min. The samples were rinsed in phosphate-buffered saline (PBS) thoroughly, before they were incubated with 100 µl of 5 µg/ml propidium iodide solution (PI, P4170, Sigma) at 37°C for 5 min. After washing with PBS three times, the samples were observed by CLSM at an excitation wavelength of 488 nm and emission wavelength of 550–670 nm.

2.7. Primary Chondrocyte Isolation and Culture

Chondrocytes were isolated from pig articular cartilage. Briefly, cartilage slices collected from femoral condyle were digested first with 0.25% TrypLE (Invitrogen) for 30 min, then with 0.25% (w/v) type-II collagenase solution (Invitrogen) in DMEM for 12–16 h at 37°C. Isolated chondrocytes were expanded in DMEM + 10% FBS. Expanded chondrocytes were seeded onto the scaffold at a density of 1×10^7 cells/ml, and cultured in chondrogenic media containing high glucose DMEM supplemented with 10^{-7} M dexamethasone, 1% ITS + premix, 50 mg/ml ascorbic acid, 1 mM sodium pyruvate, 4 mM proline and 10 ng/ml TGFβ3 (R&D Systems). The cell/scaffold composites were cultured at 37°C in 5% CO_2 over a period of up to 3 weeks. Medium was changed every 3 days.

2.8. RNA Analysis and Real-Time PCR

Total RNA was extracted with RNeasy Mini Kit (Qiagen) following the manufacturer's instructions. cDNA was reverse transcribed using the iScript™ cDNA synthesis kit (Bio-Rad), following the manufacturer's instructions. Real-time

PCR was performed using the Power SYBR Green PCR Master Mix (Applied Biosystems) on a Applied Biosystems 7500 Real-Time PCR System at 95°C for 15 min, followed by 40 cycles of 15 s denaturation at 94°C, 30 s annealing at 55°C and 30 s elongation at 72°C. Each sample was amplified three times for each gene of interest. Genes of interest were normalized to the reference gene glutaraldehyde-3-phosphate dehydrogenase (GAPDH). The level of target gene expression was calculated as $2^{-\Delta\Delta Ct}$. The following forward and reverse primers were used for amplification: for GAPDH, forward 5′-ATGGTGAAGGTCGGAGTGAA-3′, reverse 5′-AATGAAGGGGTCATTGATGG-3′; for aggrecan, forward, 5′-CATCACCGAGGGTGAAGC-3′, reverse 5′-CCAGGGGCAAATGTAAAGG-3′; for type-II collagen, forward 5′-TGAGAGGTCTTCCTGGCAAA-3′, reverse 5′-GAAGTCCCTGGAAGCCAGAT-3′.

2.9. Histological and Immunohistological Assessment

The samples were washed with PBS and embedded with Tissue Freezing Medium® (Leica, Cat. No. 020108926). Cryosections of 10 μm were prepared using a Leica Cryostat Microtome (CM3050 S). The cut sections were then fixed in an ice-cold mixture of acetone and methanol (1:1, v/v) before processing for histological and immunological staining.

For Alcian blue staining, the tissue sections were incubated with 0.5% Alcian blue (Sigma-Aldrich) in 0.1 M HCl for 30 min and counterstained with nuclear fast red (Sigma-Aldrich). For immunohistochemistry staining, endogenous peroxidase in the tissue sections was first blocked with hydrogen peroxide before pepsin treatment for 20 min. Monoclonal antibodies for type-II collagen (Clone 6B3, Chemicon) diluted factor 1:500 were applied for 1 h, followed by incubation with biotinylated goat anti-mouse (Lab Vision) for 30 min. Streptavidin peroxidase was added for 45 min, 3,3′-diaminobenzidine was used as a chromogenic agent and counterstaining was done with Gill's hematoxylin. The slides were dehydrated before coverslipping. The control mouse IgG isotype was from Zymed Laboratories.

2.10. Statistical Analysis

One-way analysis of variance (ANOVA) was used to compare the difference between each group, and all data were expressed as mean ± SD. Statistical significance was reported at the 95% confidence level ($P < 0.05$) for all tests.

3. Results

3.1. Characterization of the Scaffolds

The PLCL scaffolds acquired were three-dimensional porous structures with pore sizes ranging between 200 and 500 μm. Both the PLCL and chitosan-modified PLCL scaffolds had a porosity of roughly 85% and a homogeneously interconnected pore structure (Fig. 2). After reacting with 1,6-hexanediamine (ninhydrin staining), chitosan-modified PLCL scaffolds were stained purplish red, while the

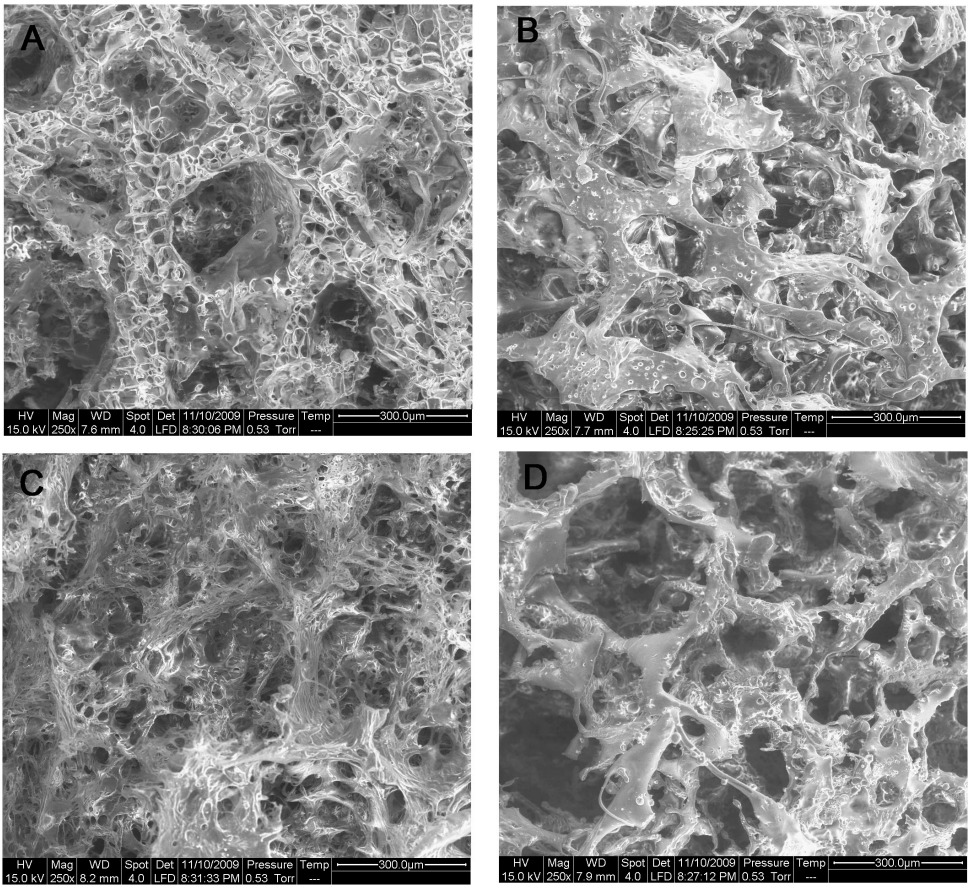

Figure 2. SEM images of a PLCL scaffold and a chitosan-modified PLCL scaffold. (A) Surface of the PLCL scaffold; (B) surface of the chitosan-modified scaffold; (C) cross-section of the PLCL scaffold; (D) cross-section of the chitosan-modified scaffold. Scale bar = 300 µm.

PLCL scaffolds were not stained. XPS also confirmed that the chitosan-modified scaffolds, but not the PLCL scaffolds, had a significant N_{1s} peak at 399.22 eV, which confirmed successful addition of N (potential amine group) (Fig. 3). The swelling ratio of chitosan-modified scaffolds increased 1.33 times ($P < 0.05$), compared with original PLCL scaffolds, mainly due to cross-linking of hydrophilic chitosan (Fig. 4).

3.2. Mechanical Characterization of the Scaffolds

3.2.1. Compression

The average stress–strain relationship under the compression of the samples to 45% strain ($n = 6$) demonstrated that both scaffolds (chitosan-modified and non-modified) had similar inhomogeneous and nonlinear properties similar to bovine cartilage (Fig. 5). The Young's compression modulus of the chitosan-modified scaf-

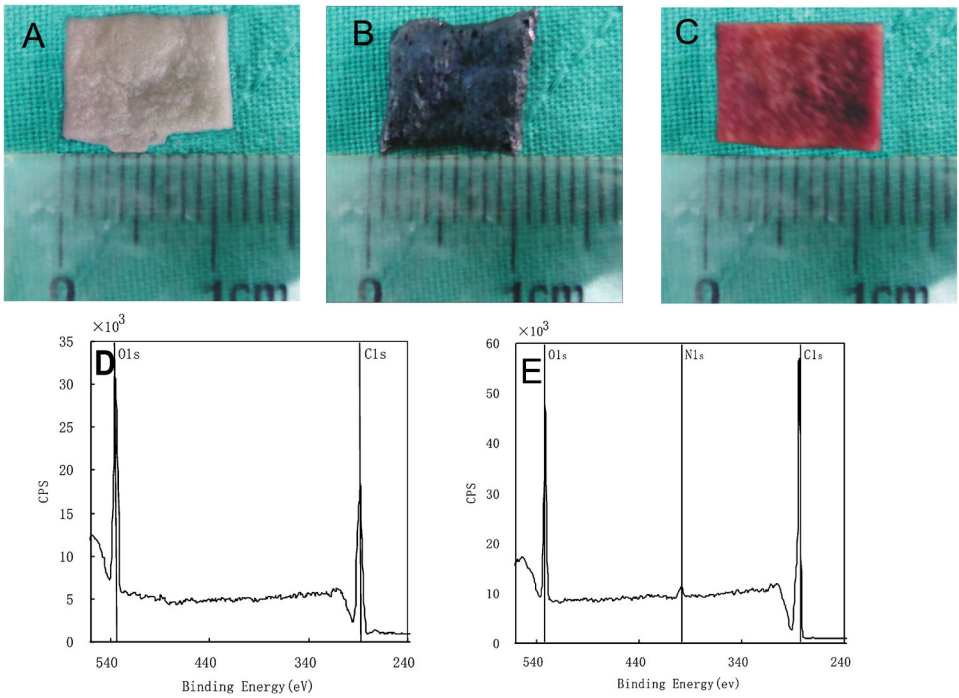

Figure 3. Ninhydrin staining and XPS data of the PLCL scaffold and the chitosan-modified scaffold. (A) Ninhydrin staining of the PLCL scaffold; (B) ninhydrin staining of the aminolysed PLCL scaffold; (C) ninhydrin staining of the chitosan-modified PLCL scaffold; (D) XPS of the PLCL scaffold; (E) XPS of the chitosan-modified PLCL scaffold. This figure is published in colour in the online edition of this journal, which can be accessed *via* http://www.brill.nl/jbs

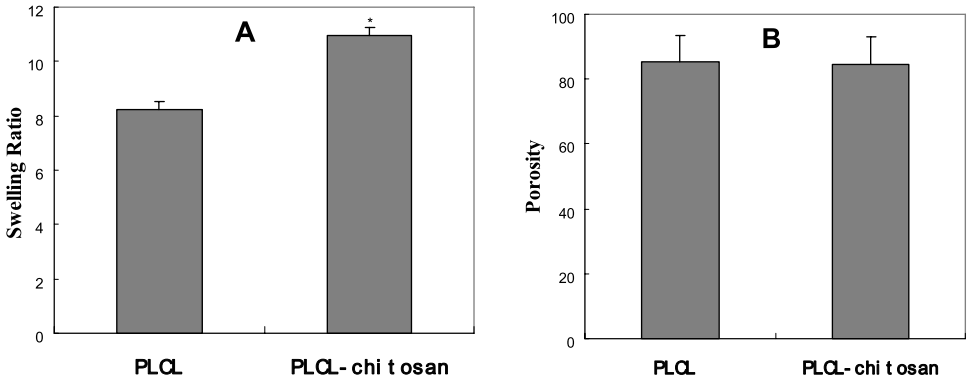

Figure 4. (A) PLCL and chitosan-modified PLCL scaffold immersed in PBS at 37°C for 2 h to determine the equilibrium swelling ratio of the scaffolds; (B) the porosity of the PLCL and chitosan-modified PLCL scaffold ($n = 4$). $^{*}P < 0.05$ compared with PLCL groups.

folds was 0.04 ± 0.01 MPa, much higher than that of PLCL scaffolds (0.02 ± 0.01 MPa) and still one magnitude less than that of bovine cartilage (0.53 ± 0.22 MPa) (Table 1). The recovery ratio (97.36%) of chitosan-modified PLCL scaf-

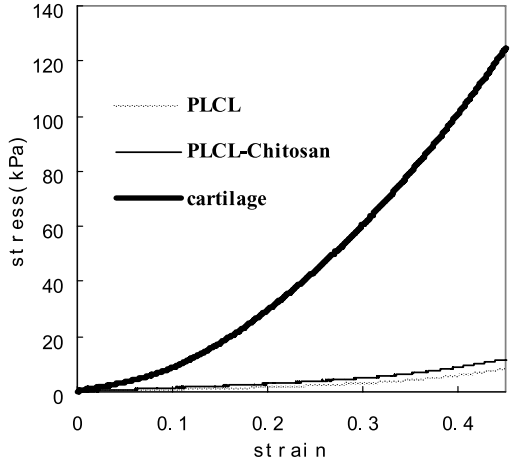

Figure 5. Compressive stress–strain curve of PLCL scaffolds, chitosan-modified PLCL scaffolds and bovine cartilage to 45% strain. Each line indicates the average stress of samples ($n = 6$).

Table 1.
Young's modulus at 45% strain in the compression test of PLCL, chitosan-modified PLCL scaffolds and bovine cartilage

	Young's modulus (MPa)	*P* value
PLCL scaffold	0.02 ± 0.01	
Chitosan-modified PLCL scaffold	0.04 ± 0.01	<0.05
Bovine cartilage	0.53 ± 0.22	<0.05

Table 2.
Recovery ratio of PLCL, chitosan-modified PLCL scaffolds and bovine cartilage from compression deformation

	Recovery ratio (%)	*P* value
PLCL scaffold	90.60 ± 4.17	<0.05
Chitosan-modified PLCL scaffold	97.36 ± 1.41	>0.05
Bovine cartilage	99.20 ± 0.65	

folds was higher than PLCL scaffolds (90.60%), while it was similar to bovine cartilage (99.20%) (Table 2).

3.2.2. Viscoelasticity

All samples showed viscoelasticity when changes in strain of the samples were analyzed with loading at 10 kPa for 300 s. As time progressed, strain of the samples increased and ultimately approached equilibrium (Fig. 6). However, chitosan-modified PLCL scaffolds achieved equilibrium faster than PLCL scaffolds and with

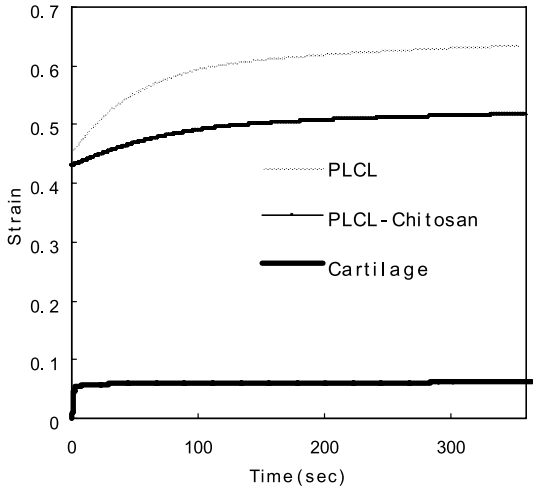

Figure 6. Changes in the strain of PLCL scaffolds, chitosan-modified PLCL scaffolds and bovine cartilage on loading (10 kPa) in a creep test. Each line indicates the average strain of samples over time ($n = 4$).

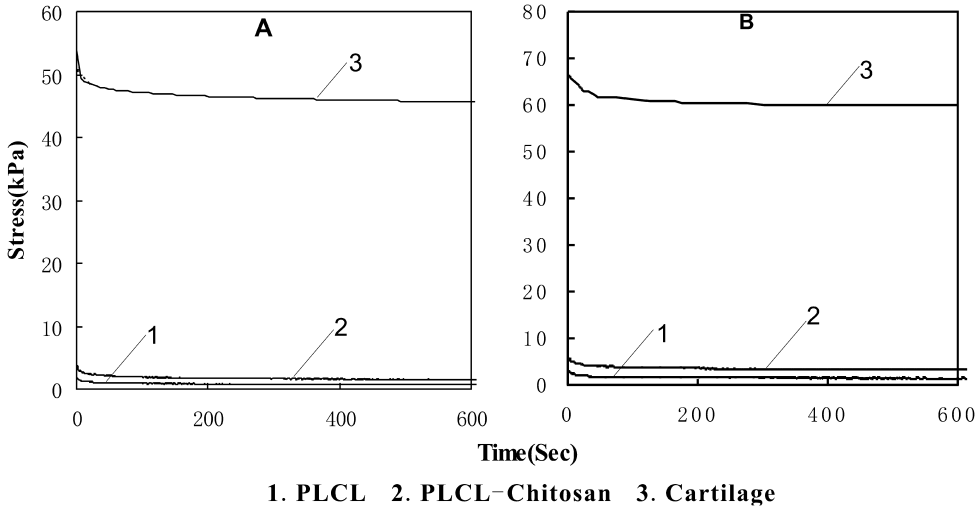

Figure 7. Stress relaxation characteristics of PLCL scaffolds, chitosan-modified PLCL scaffolds and bovine cartilage. (A) 20% strain; (B) 30% strain.

a more similar creep property to native cartilage. During the stress relaxation test of the scaffolds or cartilage, immediately generated stress gradually decreased with time and reached equilibrium stress within several hundred seconds (Fig. 7). The chitosan-modified scaffolds had more of a similar viscoelastic property to native cartilage than that of PLCL scaffolds (Figs 6 and 7).

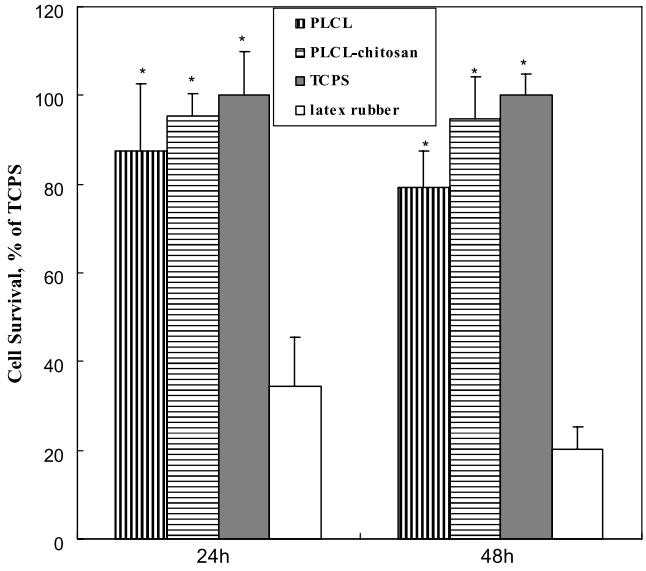

Figure 8. Biocompability of PLCL scaffolds and chitosan-modified PLCL scaffolds tested using the MTT assay. Data are expressed as the percentage of TCPS ($n = 6$). $^*P < 0.05$ compared with latex rubber groups.

3.3. Biocompatibility

Both PLCL scaffolds and chitosan-modified scaffolds showed a good biocompatibility with a similar survival rate as cells growing on a tissue-culture plate (Fig. 8). Comparatively, cells did not survive well with latex rubber ($P < 0.05$).

3.4. Attachment and Proliferation of Chondrocytes in the Scaffolds

From the DNA assay, the number of chondrocytes attached to the chitosan-modified PLCL scaffold was 1.5-times higher than that of the unmodified PLCL scaffolds at 6 h (Fig. 9). Loaded chondrocytes proliferated 1.625- and 1.774-times on PLCL and chitosan–PLCL, respectively, from 6 h to 3 days. The number of chondrocytes on chitosan-modified PLCL scaffolds was 1.67-times higher than that on the PLCL scaffolds at 3 days. The chondrocytes on the chitosan-modified scaffolds spread better, and cell numbers were higher than those on the PLCL scaffold (Fig. 10A, B). After 3 days of culture, some chondrocytes in the chitosan-modified PLCL scaffolds aggregated into clusters within the chitosan-modified scaffolds, while the chondrocytes in the PLCL scaffolds were still distributed homogeneously in the scaffolds (Fig. 10C, D).

3.5. Cartilage Tissue Formation

ECM deposition assessed by Alcian blue staining for proteoglycan and type-II collagen immunostaining showed increased deposition of these ECM proteins by chondrocytes cultured in chitosan-modified PLCL (Fig. 11). Formation of cartilage

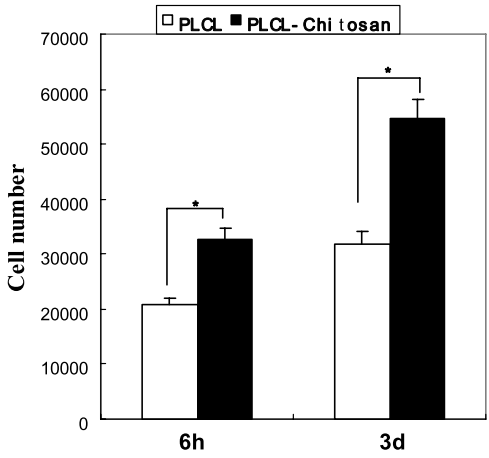

Figure 9. DNA assay applied to investigate chondrocyte attachment at 6 h after cell seeding, and proliferation at 3 days after cell seeding on PLCL and chitosan-modified PLCL scaffolds ($n = 4$). $^{*}P < 0.05$ compared with PLCL groups.

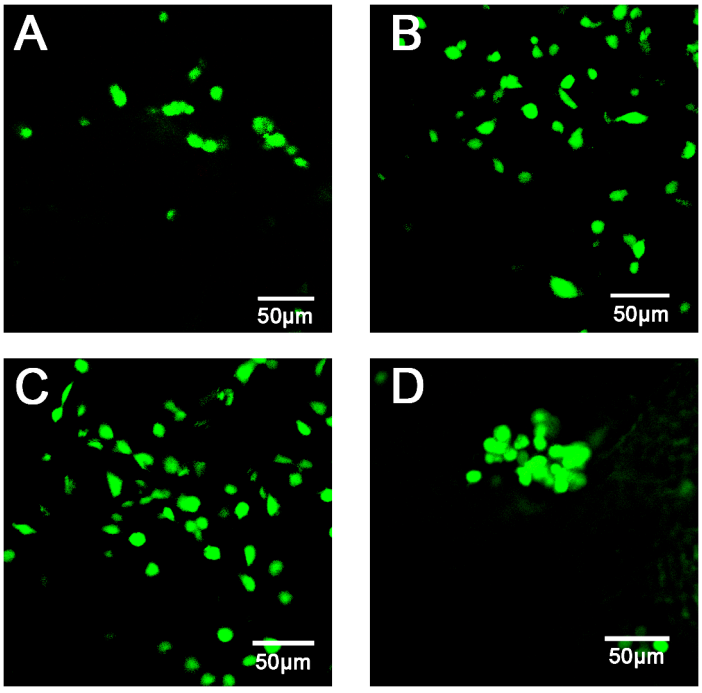

Figure 10. (A, B) CLSM images showing chondrocytes on the surface of (A) PLCL and (B) chitosan-modified PLCL scaffolds 6 h after cell seeding. (C, D) CLSM images showing chondrocytes on the surface of (C) PLCL scaffolds and (D) chitosan-modified PLCL scaffolds 3 days after cell seeding. The live cells were dyed with FDA (green) and dead cells were stained with PI (red). Cell seeding density $= 2 \times 10^5$/scaffold. This figure is published in colour in the online edition of this journal, which can be accessed *via* http://www.brill.nl/jbs

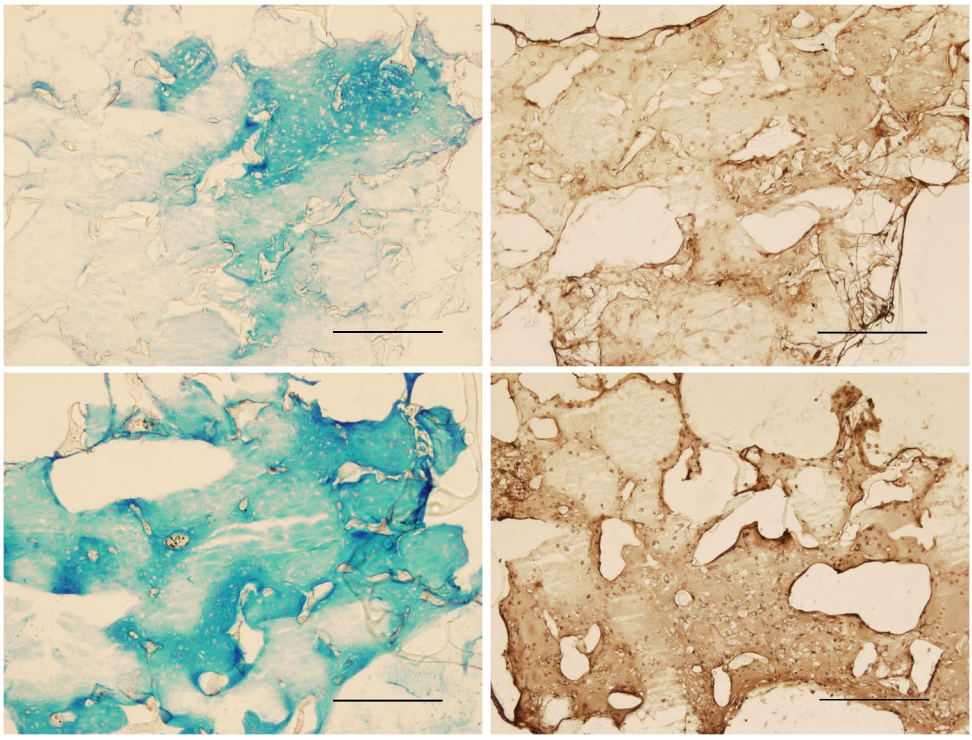

Figure 11. Histological studies of chondrocytes cultured in (a, b) PLCL or (c, d) chitosan-modified PLCL scaffolds for 3 weeks. The sections were stained with (a, c) Alcian blue or (b, d) type-II collagen. Images were taken at ×100 magnification and are representative of two experiments. This figure is published in colour in the online edition of this journal, which can be accessed *via* http://www.brill.nl/jbs

tissue was more widely spread in the chitosan-modified PLCL than in unmodified PLCL. The increase deposition of the ECM proteins was mirrored by the increase in mRNA expression of aggrecan (*Aggr*) and type-II collagen (*Col2*) as measured by real-time PCR analysis (Fig. 12). Chondrocytes expressed a 2-fold increase in *Aggr* and *Col2* ($P = 0.003$ and 0.004, respectively) after 7 days culture in chitosan-modified PLCL compared with the unmodified PLCL. The increase in cartilaginous genes expression persisted to day 14.

4. Discussion

Cartilage extracellular matrix is composed of a dense network of collagen fibrils (20% of the extracellular matrix) and a highly hydrophilic gel of proteoglycans (5% of the extracellular matrix) immobilized onto a collagen network. Proteoglycans have a large number of negatively charged glycosaminoglycan chains, which hold a great amount of water molecules. The highly concentrated and hydrophilic proteoglycans form a swelling pressure within the extracellular matrix, which is constrained by a relatively inextensible collagen network, producing resistance to

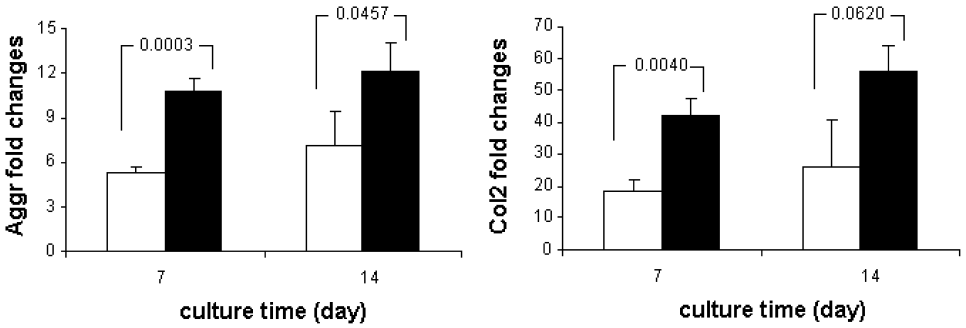

Figure 12. Real-time quantification of *Aggr* and *Col2* expression in chondrocytes cultured in PLCL (white bar) or chitosan-modified PLCL scaffolds (black bar). Expression was normalized to GAPDH and presented relative to level chondrocytes prior to seeding in scaffolds. Data shown are means ± SD ($n = 3$, representative of separate experiments from 2 pigs).

external force. Proteoglycans, collagen, as well as their interaction endow articular cartilage with the unique physical properties of reversible compression and tensile strength to withstand mechanical stress [24, 25].

There has been some success in cartilage tissue regeneration by application of various scaffolds such as chitosan, PLGA, PLCL and their composites [26–28]. Although some regenerated cartilages had a morphology similar to normal hyaline cartilage, internal structures were far from ideal. Complex mechanical properties of cartilage have not yet been achieved by any synthetic scaffold, mainly due to the scaffolds lacking biochemical components and structures of native cartilage. Cyclic mechanical stimulus has been reported to promote cartilage regeneration *in vitro* and *in vivo*. Based on that observation, mechano-active scaffolds have been fabricated in an aim to optimize structures of neo-cartilage by transferring proper mechanical stimuli to individual cells and the extracellular matrix [15, 29, 30]. A highly elastic PLCL scaffold has been reported to provide good mechanical strength over a certain period of time until neocartilage is regenerated; however, the hydrophobic PLCL scaffolds could not provide biological recognition sites for cell adhesion and lacked appropriate stiffness to withstand external force [13, 15].

Some strategies have been adopted to optimize physical/chemical microenvironments of polyesters, such as increasing surface roughness [31] and hydrophilicity, or immobilization of a biocompatible macromolecular layer on the surface. A biomimetic porous scaffold was made of a biodegradable graft copolymer chondroitin sulfate-grafted poly(L-lactide) (CS–PLLA) by introducing chondroitin sulfate, a natural component of cartilage. Structures of the biomimetic scaffolds were different from cartilage, as both PLLA and CS–PLLA were simply mixed with each other [32]. Inspired by the success of biomimetic biomaterials, we propose that viscoelastic scaffolds could be made through biphasic materials mimicking native cartilage [33, 34]. Chitosan has been broadly applied to tissue engineering due to its relatively good biocompatibility and ease of usage. Chitosan can be regarded as a biochemical counterpart of glycosaminoglycans (GAGs, main components

of proteoglycan) due to its similar hexose consisting of water-soluble structural units. PLCL is a highly elastic synthetic macromolecular compound which simulated an elastic collagen fiber network in native cartilage. It was chosen in place of the broadly adopted PLA and PLGA, mainly due to its intrinsic elasticity. Furthermore, when PLCL degrades into relatively mild acidic products compared to PLGA, chitosan could neutralize the acidic products from the degradation of PLCL. In the current study, chitosan was immobilized onto the PLCL scaffold by aminolysis methods to simulate the biochemical components of the cartilage extracellular matrix [22, 35]. In the aminolysis process, ester groups of PLCL backbone reacted with one amino group of 1,6-hexanediamine to form a covalent bond while the other amino group remained free to cross-link with chitosan through glutaraldehyde. Successful cross-linking of chitosan to PLCL was confirmed by ninhydrin staining and XPS, which qualitatively showed presence of the NH_2 group in the scaffolds [27, 36, 37].

Practically, the chitosan-modified PLCL scaffolds could possess mechanical properties similar to native cartilage. Under compression stress, water molecules held by ionic groups of chitosan inside the scaffolds would endow the scaffolds with viscoelasticity following a similar principle found within native cartilage. An increase in viscoelasticity of the chitosan–PLCL scaffolds was confirmed by the creep and stress relaxation test. Usually aminolysised PLCL scaffolds should have a lower stiffness than PLCL scaffolds due to fragmentation of the PLCL macromolecular chain, but in the current study, both the Young's modulus and recovery ratio of chitosan-modified scaffolds increased compared to unmodified PLCL scaffolds. It is likely that the cross-link of chitosan has increased the internal stiffness of the structures. Although the Young's modulus of the chitosan-modified PLCL scaffolds was higher than that of unmodified PLCL scaffolds, it was still one order of magnitude less than bovine cartilage. To date, the most successful scaffolds, regarding mechanical properties, are poly(glycolic acid) (PGA) woven structures mixed with hydrogels [18]. The current chitosan-modified PLCL scaffolds have a Young's modulus similar to the composite scaffold as mentioned above (0.005 and 0.1 MPa). While both the scaffolds did not have sufficient stiffness/Young's modulus to fully withstand applied high stress, the deformation recovery ratio of chitosan-modified PLCL scaffolds (97.36%) was in a range very similar to native cartilage and could potentially deliver proper physiological mechanical signals to the attached chondrocytes.

Differences in biochemical components and physical/chemical properties lead to disparities in mechanical properties between scaffolds and native cartilage. When stress is loaded on the native cartilage, the forces generated from the native cartilage, including the fluid flow and osmotic pressure derived from the interaction of ions with the proteoglycans, can balance external forces. In the current study, when chitosan-modified PLCL scaffolds were loaded in a PBS-immersed environment, hydrophilic NH_2 groups within the scaffolds absorbed large amounts of water resulting in a relatively high osmotic pressure to resist external pressure.

Multiple causes contribute to the mechanical differences between the biomimetic scaffolds and native cartilage. Firstly, structures of biomacromolecules in cartilage and scaffolds are different. In cartilage, three collagen molecules self-assemble into a collagen fiber with natural triple-helical domains and eventually form the sequential arrangement of collagen fibrils, which brings about the high elasticity of collagen network while the PLCL molecules of current scaffolds are in a disordered structure. Secondly, electronegative aggrecans in cartilage are cross-linked into the collagen network; however, in the current biomimetic scaffolds inexpensive and electropositive chitosan was covalently bonded only to the surface of PLCL scaffold. Thirdly, the ratio of chitosan and PLCL in the current scaffolds is not the same as that of aggrecan and collagen in native cartilage. Therefore, there is still room to improve the mechanical properties of current biomimetic scaffolds through further chemical engineering. In the current study, chitosan-modified PLCL scaffolds had a good recovery ratio similar to native cartilage, which could possibly supply a mechanically compatible microenvironment for cell adhesion, proliferation and differentiation.

It has been known that biochemical components of biomaterials are critical for potential chondrogenesis [38]. More chondrocytes attached to the chitosan-modified PLCL scaffolds than to the unmodified scaffolds, which can be attributed to a fairly good biocompatibility of chitosan. It is also evidenced by enhanced gene expression and extracellular matrix excretion of aggrecan and type-II collagen of chondrocytes within chitosan-modified PLCL scaffolds, compared with PLCL scaffolds. Chondrocytes spread better when compared with unmodified PLCL scaffolds at 6 h. Interestingly, a majority of chondrocytes on the chitosan-modified PLCL scaffolds aggregated as clusters after 3 days, in contrast to chondrocytes on the PLCL scaffolds which were distributed homogeneously. As proper aggregation is critical for chondrocyte function and chondrogenesis, chitosan may help to promote chondrogenesis through regulating proper chondrocyte aggregation [39].

The main purpose of this study was to design viscoelastic three-dimensional porous scaffolds that simulate the structure and components of native cartilage. Current scaffolds are biocompatible as well as biodegradable and could provide a good microenvironment for cell adhesion, proliferation and extracellular matrix excretion. They are potentially good for cartilage regeneration by providing proper mechanical and biochemical signals for chondrocyte adhesion and differentiation. In a future study, efforts should be made to improve stiffness of the chitosan-modified PLCL scaffolds through different chemical modifications while studying the mechanical properties of the resulting cartilage tissue. The mechanism of cell aggregation induced by chitosan should also be further investigated.

5. Conclusions

Current chitosan-modified PLCL scaffolds have similar viscoelastic properties with native cartilage, a good recovery ratio and relatively good biocompatibility for tis-

sue engineering and regeneration. With the design of similar internal structures and components of native cartilage, the mechanical properties of the scaffolds can be further improved to meet the requirements for both research and clinical applications. The scaffolds could not only serve as a model for cell mechanical study but could also be directly implanted *in vivo* as a cellular inductive, as well as a supporting structure.

Acknowledgements

This study was supported by the National Natural Science Foundation of China (grants 30970881 and 31011140348) and a Seed Grant from the Wallace H. Coulter Foundation. The authors thank Song Yun for assistance with environmental scanning electronic microscope and Prof. Chun Yang for advice on the mechanical test. The authors also thank Dr. Mary Goldring for kindly providing the chondrocyte line C28-I2. The authors declare they have no competing interests.

References

1. L. A. Setton, D. M. Elliott and V. C. Mow, *Osteoarthr. Cartil.* **7**, 2 (1999).
2. M. Brittberg, A. Lindahl, A. Nilsson, C. Ohlsson, O. Isaksson and L. Peterson, *N. Engl. J. Med.* **331**, 889 (1994).
3. L. Hangody, G. Vasarhelyi, L. R. Hangody, Z. Sukosd, G. Tibay, L. Bartha and G. Bodo, *Injury* **39** (Suppl. 1), S32 (2008).
4. Y. N. Wu, Z. Yang, J. H. Hui, H. W. Ouyang and E. H. Lee, *Biomaterials* **28**, 4056 (2007).
5. M. H. Zheng, C. Willers, L. Kirilak, P. Yates, J. Xu, D. Wood and A. Shimmin, *Tissue Eng.* **13**, 737 (2007).
6. F. Ito, K. Usui, D. Kawahara, A. Suenaga, T. Maki, S. Kidoaki, H. Suzuki, M. Taiji, M. Itoh, Y. Hayashizaki and T. Matsuda, *Biomaterials* **31**, 58 (2010).
7. D. A. Wang, S. Varghese, B. Sharma, I. Strehin, S. Fermanian, J. Gorham, D. H. Fairbrother, B. Cascio and J. H. Elisseeff, *Nature Mater.* **6**, 385 (2007).
8. Y. Jung, S. H. Kim, S. H. Kim, Y. H. Kim, J. Xie, T. Matsuda and B. G. Min, *J. Biomater. Sci. Polymer Edn* **19**, 61 (2008).
9. C. G. Jeong and S. J. Hollister, *Biomaterials* **31**, 4304 (2010).
10. V. Kesireddy, J. Ringe, M. Endres, S. Stich, D. Klose, R. Bodmeier and M. Sittinger, *Tissue Eng.* **12**, 1073 (2006).
11. C. W. Lou, C. H. Yao, Y. S. Chen, T. C. Hsieh, J. H. Lin and W. H. Hsing, *Textil. Res. J.* **78**, 958 (2008).
12. Y. Jung, S. H. Kim, H. J. You, S. H. Kim, Y. H. Kim and B. G. Min, *J. Biomater. Sci. Polymer Edn* **19**, 1073 (2008).
13. S. I. Jeong, B. S. Kim, Y. M. Lee, K. J. Ihn, S. H. Kim and Y. H. Kim, *Biomacromolecules* **5**, 1303 (2004).
14. Y. Kang, J. Yang, S. Khan, L. Anissian and G. A. Ameer, *J. Biomed. Mater. Res. A* **77**, 331 (2006).
15. J. Xie, M. Ihara, Y. M. Jung, I. K. Kwon, S. H. Kim, Y. H. Kim and T. Matsuda, *Tissue Eng.* **12**, 449 (2006).
16. G. R. Ragetly, G. J. Slavik, B. T. Cunningham, D. J. Schaeffer and D. J. Griffon, *J. Biomed. Mater. Res. A* **93**, 46 (2010).

17. J. K. Suh and H. W. Matthew, *Biomaterials* **21**, 2589 (2000).
18. F. T. Moutos, L. E. Freed and F. Guilak, *Nature Mater.* **6**, 162 (2007).
19. S. Tepic, T. Macirowski and R. W. Mann, *Proc. Natl. Acad. Sci. USA* **80**, 3331 (1983).
20. L. A. Setton, W. B. Zhu and V. C. Mow, *J. Biomech.* **26**, 581 (1993).
21. M. H. Ho, P. Y. Kuo, H. J. Hsieh, T. Y. Hsien, L. T. Hou, J. Y. Lai and D. M. Wang, *Biomaterials* **25**, 129 (2004).
22. Y. B. Zhu, C. Y. Gao, X. Y. Liu, T. He and J. C. Shen, *Tissue Eng.* **10**, 53 (2004).
23. X. Liu and P. X. Ma, *Biomaterials* **30**, 4094 (2009).
24. P. J. Basser, R. Schneiderman, R. A. Bank, E. Wachtel and A. Maroudas, *Arch. Biochem. Biophys.* **351**, 207 (1998).
25. J. K. Suh and M. R. DiSilvestro, *J. Appl. Mech. Trans. ASME* **66**, 528 (1999).
26. Y. Jung, M. S. Park, J. W. Lee, Y. H. Kim, S. H. Kim and S. H. Kim, *Biomaterials* **29**, 4630 (2008).
27. D. L. Nettles, S. H. Elder and J. A. Gilbert, *Tissue Eng.* **8**, 1009 (2002).
28. K. Uematsu, K. Hattori, Y. Ishimoto, J. Yamauchi, T. Habata, Y. Takakura, H. Ohgushi, T. Fukuchi and M. Sato, *Biomaterials* **26**, 4273 (2005).
29. S. Even-Ram, V. Artym and K. M. Yamada, *Cell* **126**, 645 (2006).
30. V. Vogel and M. Sheetz, *Nature Rev. Mol. Cell Biol.* **7**, 265 (2006).
31. T. W. Chung, D. Z. Liu, S. Y. Wang and S. S. Wang, *Biomaterials* **24**, 4655 (2003).
32. C. T. Lee, C. P. Huang and Y. D. Lee, *Biomacromolecules* **7**, 2200 (2006).
33. K. A. Athanasiou, M. P. Rosenwasser, J. A. Buckwalter, T. I. Malinin and V. C. Mow, *J. Orthop. Res.* **9**, 330 (1991).
34. W. C. Hayes and L. F. Mockros, *J. Appl. Physiol.* **31**, 562 (1971).
35. Y. B. Zhu, K. S. Chian, M. B. Chan-Park, P. S. Mhaisalkar and B. D. Ratner, *Biomaterials* **27**, 68 (2006).
36. Y. C. Kuo and I. N. Ku, *Biomacromolecules* **9**, 2662 (2008).
37. J. K. F. Suh and H. W. T. Matthew, *Biomaterials* **21**, 2589 (2000).
38. J. K. Mouw, N. D. Case, R. E. Guldberg, A. H. Plaas and M. E. Levenston, *Osteoarthr. Cartil.* **13**, 828 (2005).
39. D. R. Albrecht, G. H. Underhill, T. B. Wassermann, R. L. Sah and S. N. Bhatia, *Nature Methods* **3**, 369 (2006).